End-to-End Demonstration of Fiber-Wireless Fronthaul Networks Using a Hybrid Multi-IF-Over-Fiber and Radio-Over-Fiber System

Hsuan-Yun Kao, Shota Ishimura, Kazuki Tanaka, Kosuke Nishimura, and Ryo Inohara

***Abstract*—This paper reports an end-to-end demonstration of a fiber-wireless mobile fronthaul (MFH) network based on hybrid intermediate-frequency-over-fiber (IFoF) and radio-over-fiber (RoF) links using a 28-GHz millimeter-wave (MMW) band. We successfully transmitted 24 64-QAM OFDM signals with a total bandwidth of 9.12 GHz over 20-km broadband IFoF, 1-km narrow-band IFoF, 500-m RoF, and 10-m free-space links with an aggregate capacity of up to 34.2 Gbps, which complies with the required peak data capacity of IMT-2020. A digital demultiplexer was exploited to flexibly perform channel selection and frequency conversion. The obtained results show the feasibility of implementing fiber-wireless systems with the hybrid IFoF/RoF links for future mobile fronthaul networks.**

***Index Terms*—IF-over-fiber, Radio-over-fiber, Mobile fronthaul.**

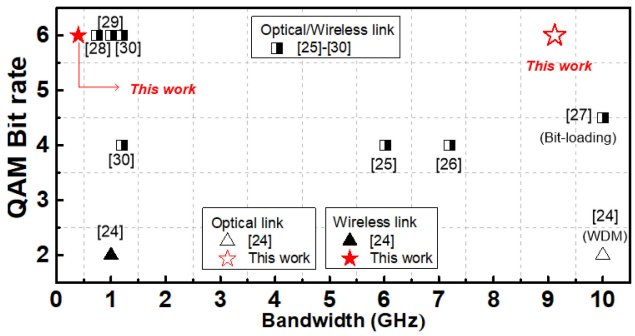

Fig. 1. QAM order versus aggregated bandwidth of recently reported fiber-wireless transmission experiments.

I. Introduction

THE volume of mobile data traffic has grown explosively to support numerous emerging applications, such as 4K video streaming, augmented/virtual reality (AR/VR) technologies, and low-latency Internet services [1], [2]. According to IMT-2020, the fifth-generation (5G) system is expected to provide a data capacity as high as 20 Gbps per cell and reduce end-to-end latency to less than 1 ms [3]–[5]. In mobile networks, on the other hand, a centralized radio access network (C-RAN) architecture has been adopted to accommodate connectivities between central units (CUs) and distributed units (DUs) [6], [7]. In this architecture, digital fiber-optic interfaces such as common public radio interface (CPRI) have been widely employed. [8]–[10]. Nevertheless, it is recognized that transmission of the digitalized signal requires a much larger capacity than the original throughput (about 16-fold larger). This will result in extremely high-capacity fronthauling in 5G and beyond [11]. Therefore, several solutions have been actively studied to improve the bandwidth issue. One approach is to change the functional-split point between CU and DU to a higher layer. For example, the 3rd Generation Partnership Project (3GPP) defines eight options for the functional split. Although this solution indeed reduces transmission capacity [12], [13], it sacrifices inter-cell interference coordination [14].

In contrast, it is possible for analog transport technology such as radio-over-fiber (RoF) and intermediate- frequency-over-fiber (IFoF) systems to retain coordination since all RAN protocols can gather at a CU. In addition, it resolves the bandwidth issue at the same time because the original waveform of a radio signal can be transmitted without digitization. Therefore, high-speed electrical and optical components are no longer required in the analog system [15], [16]. To date, several transmission experiments using the RoF/IFoF system have been conducted to investigate the feasibility of analog mobile fronthaul (MFH) links [17]–[23]. For example, [21] demonstrated IFoF transmission over 1 km with a CPRI-equivalent capacity of up to 400 Gbps by using digital signal processing (DSP)-based channel aggregation. In the demonstration, the total aggregated bandwidth was 10 GHz (32 $\times$ 200MHz). By employing a frequency converter and channel selector, [7] demonstrated IFoF transmission with a capacity of up to 24 Gbps (18 $\times$ 0.36 GHz). Moreover, [22] successfully demonstrated a CPRI-equivalent capacity of 1 Tbps using a parallel intensity/phase modulation (IM/PM) transmitter. However, all these studies focused solely on fiber transmission. On the other hand, several studies have shown the feasibility of a hybrid fiber/wireless system. Fig. 1 summarizes state-of-the-art fiber-wireless demonstrations reported so far [24]–[30]. Argyris *et al.* demonstrated a fiber-wireless system with a data rate of 24 Gbps. In the demonstration, a multiband 16-QAM single-carrier

Manuscript received July 2, 2021; revised August 9, 2021; accepted August 19, 2021. Date of publication August 24, 2021; date of current version September 3, 2021. This work was supported by the R&D contract Wired-and-Wireless Converged Radio Access Network for Massive IoT Traffic JPJ000254 with the Ministry of Internal Affairs and Communications, Japan, for radio resource enhancement. *(Corresponding author: Shota Ishimura.)*

The authors are with the KDDI Research Inc., Fujimino-shi 356-8502, Japan (e-mail: hsuan-yun.kao@nokia.com; sh-ishimura@kddi-research.jp; au-tanaka@kddi-research.jp; nish@kddi-research.jp; rinohara@kddi-research.jp).

Digital Object Identifier 10.1109/JPHOT.2021.3106706

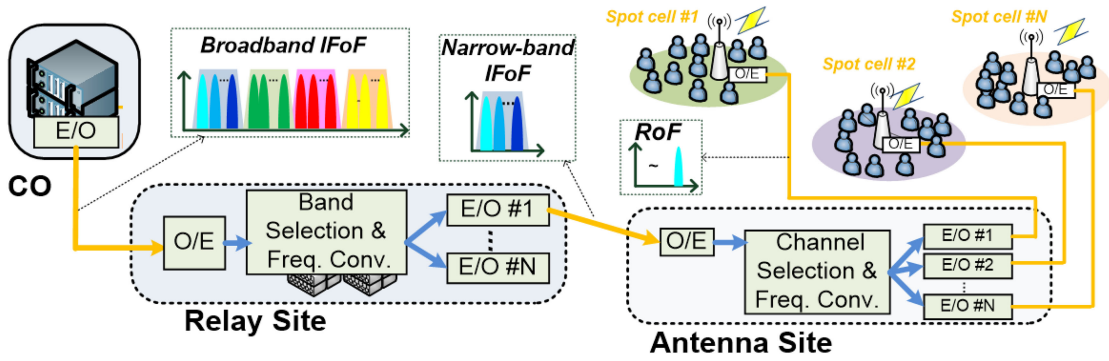

Fig. 2. Architecture of the IFoF/A-RoF hybrid MFH.

signal consisting of six 1.2-GHz signals was transmitted over 7-km SMF and 5-m wireless links [26]. Filgueiras *et al.* demonstrated 64- and 256-QAM fronthaul transmission, including 25-km SMF and 10-m wireless links at 28 and 7.5 GHz [30].

In this paper, we report on a demonstration of end-to-end fiber/wireless transmission using the IFoF system. In Ref. [7], we have already reported transmission experiments including cascaded IFoF links. In the demonstration, we transmitted multiple IF signals aggregated in the IF domain, and then they were de-aggregated using an FPGA-based demultiplexer. The digital demultiplexing process included channel extraction using a finite-impulse-response (FIR) filter and frequency conversion to a low-frequency region. Since such a digital filter makes it possible to extract an objective signal sharply, we can densely aggregate signals, which significantly improves the spectral efficiency. However, we could not demonstrate an end-to-end system including wireless transmission at 28 GHz in the experiment. Since 5G is fully utilizing the 28-GHz band, it is important to show the feasibility of the entire system including wireless transmission. Therefore, in this paper, we extend our previous work by adding 28-GHz wireless transmission to show the feasibility. In addition, we further enhance the total aggregated bandwidth to 9.12 GHz (24×0.38 GHz). As a result, we could achieve 34.2 Gbps. We believe that these results provide a deeper insight into fronthaul system design.

II. Architecture of Hybrid IFoF and RoF MFH

Fig. 2 shows the architecture of the hybrid IFoF/RoF MFH system. At a central office (CO), multiple radio signals are aggregated in the IF domain and transmitted to a relay site. We refer to this link as a broadband IFoF link. In the relay site, then, the aggregated IF signals are separated into several groups. (In Fig. 2, they are grouped into four.) Since we assume that the broadband IFoF link delivers aggregated IF signals with a total bandwidth of > 10 GHz, each group is assumed to have a bandwidth of > 2.5 GHz. In the second link, each group is transmitted to an antenna site in a different location. It should be noted that if we directly connect antenna sites to CO, numerous long optical fibers need to be installed, which is obviously an expensive solution; however, in this architecture, since a single fiber can be shared by transmitting multiple signals to a specific location, we can reduce the deployment cost associated with fiber installations. Of course, wavelength division multiplexing (WDM) can also support such a point-to-multipoint architecture [31]. Especially coarse (C)WDM offers a simpler solution when the number of antenna sites is small. However, if it increases, WDM does not necessarily provide a simple solution. For example, when the number of antenna sites is 100, we need to prepare 100 WDM channels. This is the case with massive MIMO and multi-user (MU-)MIMO scenarios in beyond-5G/6G systems. However, this number is almost comparable to submarine systems, and the WDM solution is no longer a cost-effective solution in this case. On the other hand, we can reduce the number of WDM channels with the proposed architecture by delivering multiple channels in a single wavelength. It should also be noted that before the second link, each group needs to be extracted from all the aggregated signals and down-converted to a low-frequency region to reduce the required bandwidths in the second link. For this purpose, analog band-pass filters and mixers are necessary for the relay sites. Therefore, guard bands between the adjacent groups need to be established for the analog process. Then, each group is transmitted to an antenna site. We refer to this second link as a narrow-band IFoF link. At an antenna site, a single IF signal is extracted from the group. In the extraction process, we can utilize DSP technology to provide a sharp transition filter, which enables us to aggregate the IF signals more densely. Consequently, the spectral efficiency can be improved. Moreover, since the bandwidth of the second link is relatively narrow compared to the broadband IFoF link, it becomes possible to employ off-the-shelf analog-to-digital converters (ADCs) and digital-to-analog converters (DACs). Finally, the selected signal is up-converted to a radio frequency (e.g., 28 GHz) and transmitted to a spot cell through an RoF link.

We should note that the performance of such a multi-stage system easily deteriorates especially at analog frequency conversion stages in the relay site. However, this possible degradation can be minimized by utilizing DSP at the relay site as well as at antenna sites. Since we have almost no degradation at the DSP stage as long as an ADC captures or a DAC generates waveforms with a sufficiently high vertical resolution. Although in the above discussion, at the relay site we assume the use of analog devices instead of expensive high-speed digital devices, we believe that

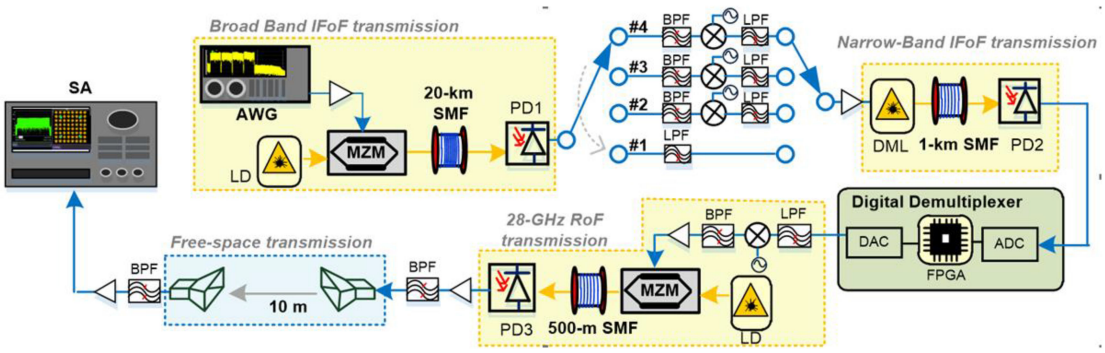

Fig. 3. Experimental setup for the hybrid end-to-end IFoF/A-RoF wireless system.

the technological evolution of electronics can potentially solve the cost issue of such high-speed digital devices, and they will be available shortly at low costs. Therefore, by utilizing them, we can implement a high-fidelity multi-stage analog fronthaul. It should also be noted that the proposed system can readily fit in a 5G system. Although digital demultiplexers need to be installed separately from CO, all RAN protocols still stay at CO, and thus the proposed system can still be regarded as a full C-RAN architecture. In addition, since digital demultiplexers can be operated independently of RAN protocols, the proposed system has no impact on RAN architectures and passively convey analog waveforms to antenna sites.

In the discussion so far, we assume a downlink architecture. On the other hand, we have recently proposed an uplink architecture [32]. In the proposed system, we assign the C-band to a downlink and the O-band to an uplink. Since such a bi-directional system has already been commercialized in a lot of applications (e.g., passive optical networks), it should readily be implemented at a low cost.

III. Experimental Setup

Fig. 3 shows the experimental setup for a hybrid IFoF/A-RoF wireless system consisting of a 20-km SMF (for the broadband IFoF link), 1-km SMF (for the narrow-band IFoF link), 500-m SMF (for the final RoF link), and 10-m free space. First, we generated a 5G OFDM signal using a Keysight 5G new radio (NR) generator. The signal contained 2640 subcarriers modulated in 64 QAM and 528 pilot subcarriers modulated in QPSK. Since the fast-Fourier-transform (FFT) size and the subcarrier spacing were set to be 4096 and 120 kHz, respectively, the total bandwidth was 380.16 MHz. We generated 24 OFDM signals with the same parameters and divided them into four groups. (#1-6, #7-12, #13-18, and #19-24). The start frequencies of the groups were set to be 0.1, 3.1, 6.1, and 9.1 GHz, respectively. Therefore, the total bandwidth of the aggregated signal became around 11.5 GHz. Then we loaded the signal to an arbitrary waveform generator (AWG) operating at 50 GS/s. At the first broadband IFoF link, the electrical output was amplified by an RF amplifier and injected into a Mach-Zehnder modulator (MZM). The MZM was operated at the C-band. Then, the modulated optical signal was transmitted over a 20-km SMF and detected by the first photodiode (PD1). Subsequently, the received 24 channels were separated into four groups. While the first group was extracted using just a low-pass filter, the other groups were down-converted to the same frequency region from 0–3 GHz after extraction using a band-pass filter.

In the second narrow-band IFoF link, a 10-GHz-class directly modulated laser (DML) was used as a transmitter. The DML was operated at the optimized bias current of 35 mA. The narrow-band IFoF signal was then transmitted over a 1-km SMF to an antenna site and detected by the second PD (PD2). At the antenna site, the signal selection was performed using a digital demultiplexer. The demultiplexer included a field-programmable gate array (FPGA) board, ADC, and DAC. In the FPGA board, the filtering and down-conversion processes were implemented. Since the DAC bandwidth was $>$ 0.8 GHz, the demultiplexer could output two IF signals (2CC) at maximum (i.e., 2 x 380.16 MHz). We could also flexibly select the number of output IF signals (either one or two) from the FPGA. Note that the latency occurring in the DSP stage was measured to be 2.8 us [7]. The output from the demultiplexer was up-converted to 28 GHz and injected into another MZM. The light source was at the C-band. Then, the signal was transmitted over a 500-m SMF over a final RoF link and detected by a high-speed PD (PD3). At a spot cell, the 1CC (or 2CC) signal at 28 GHz was amplified by a low-noise amplifier (LNA) and emitted into the air by a horn antenna over a 10-m free space. On the user equipment (UE) side, the 28-GHz signal was received by another horn antenna and amplified using an LNA to compensate for the power loss occurring during free-space transmission. Finally, the signal was captured by a spectrum analyzer (SA) and analyzed using 5G NR software installed in the SA. We analyzed the error-vector-magnitude (EVM) values of all 24 channels using the software. It should be noted that the group selection was performed by manually changing analog filters and mixers, as shown in Fig. 3. On the other hand, we could programmably select one of the six signals (or two of six signals) using the FPGA. It should also be noted that we performed pre-emphasis to flatten the EVM values based on the frequency responses of the broadband IFoF link.

IV. Results and Discussion

Fig. 4(a) shows the RF spectra in the electrical back-to-back (BtB) state and after the broadband IFoF link (with and without pre-emphasis). The EVM performance in each condition is also

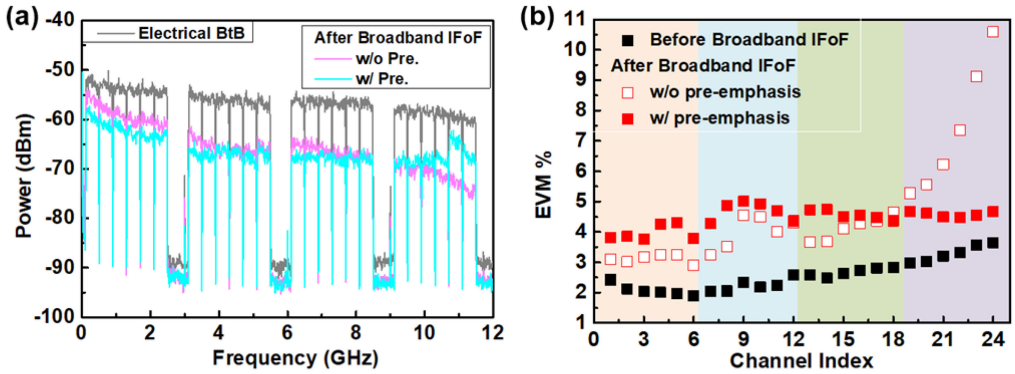

Fig. 4. (a) The received RF spectra and (b) EVM performance of broadband IFoF link after electrical BtB and broadband IFoF transmission.

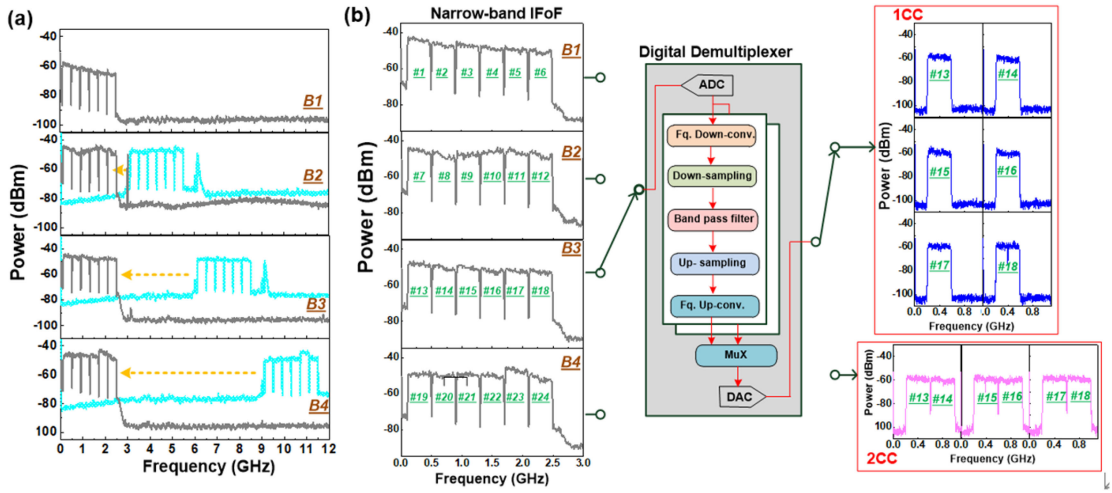

Fig. 5. The RF spectra of (a) the narrowband signal before/after analog band demultiplexer and (b) before/after digital channel demultiplexer for 1CC/2CC IF channel transmission.

plotted in Fig. 4(b). It is found from these figures that the fourth IF band incurred greater degradation. This is mainly attributed to dispersion-induced power fading. However, after performing pre-emphasis, the EVM values could be flattened, as shown in Fig. 4(b). On the other hand, Figs. 5(a) and (b) show the RF spectra of the four groups at the relay site before and after the digital demultiplexer. (It shows the spectra of channels from #13 to #18 as an example.) In the demultiplexing process, EVM degradations were found to be around 0.2%. Note that there was no significant EVM difference between the 1CC and 2CC cases. Fig. 6(a) shows the measured EVM values at all points. It was found that the average EVMs after up-conversion to 28 GHz were degraded from 6.2%, 6.6%, 6.6%, 6.5% to 7.1%, 7.3%, 7.3%, 7.3% in the first, second, third, and fourth bands, respectively. This was attributed to a large conversion loss in the analog mixing process. In addition, at this stage, an EVM difference of 0.1% between the 1CC and 2CC cases was observed due to the bandwidth limitation of the mixer.

Next, we show the performance of the 28-GHz RoF transmission. After the 500-m RoF link, the average EVMs in the 1CC and 2CC cases were observed to be 6.7% and 7.8%, respectively. Note that the received optical power was set at an optimal point of 1 dBm. However, the EVMs of channel #10, #14, #16, #19, #20 and #24 in the 2CC case failed to meet the 8% EVM requirement of 64QAM. The was attributed to the frequency response of the DACs in the digital demultiplexer. Therefore, we only conducted wireless transmission for the 1CC condition since the EVMs of some RF channels in the 2CC case already exceeded 8%. (If we can extend the bandwidth DACs, it becomes possible to improve the EVM for the 2CC condition.) Fig. 6(b) shows a photograph of an anechoic chamber in which we conducted the 10-m free-space transmission experiment. It was found from Fig. 6(a) that the EVMs of all 24 channels after the 10-m free-space transmission in the 1CC case were below 8%. In this case, the downlink transmission capacity was 24 (IF channels) $\times$ 0.38 GHz (channel bandwidths) $\times$ 3.75 bit/s/Hz (spectral efficiency) $=$ 34.2 Gbps. To discuss the system sensitivity and budget in detail, we show the EVM curves as a function of received optical power for channels #1 and #24 in Fig 6 (c). The received powers of -3.3 and -2.1 dBm were needed to satisfy the 3GPP requirement for channels #1 and #24, respectively. In addition, the power budgets were 3.8 and 2.9 dB for channels #1 and channel #24.

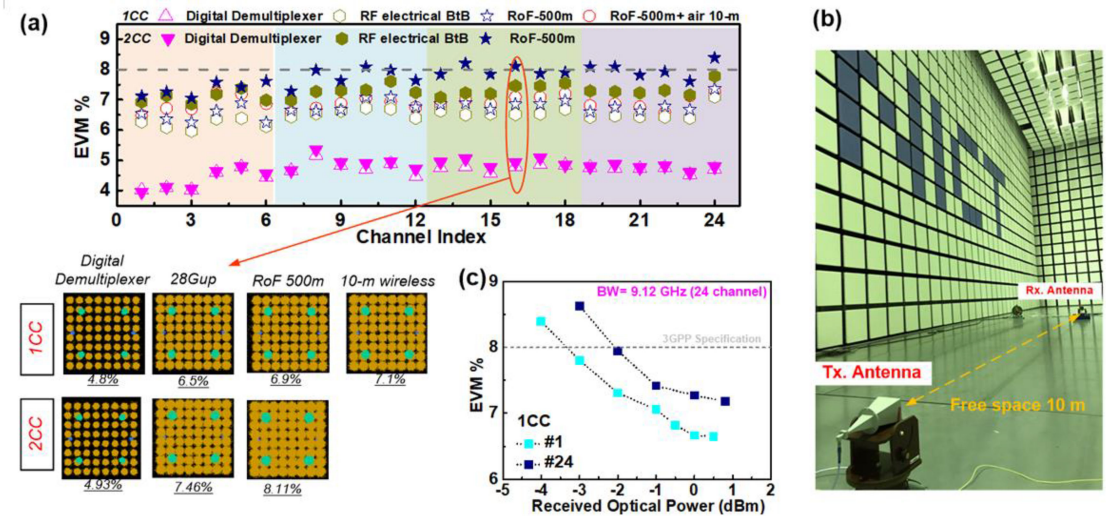

Fig. 6. (a) EVM performances and constellation plots after the digital demultiplexer, after the 28-GHz up-conversion, after the 500-m RoF transmission, and after the 10-m wireless transmission. (b) View of the experiment test bench, and Tx./Rx. terminals in an anechoic chamber. (c) EVMs as a function of received optical power for channels #1 and #24.

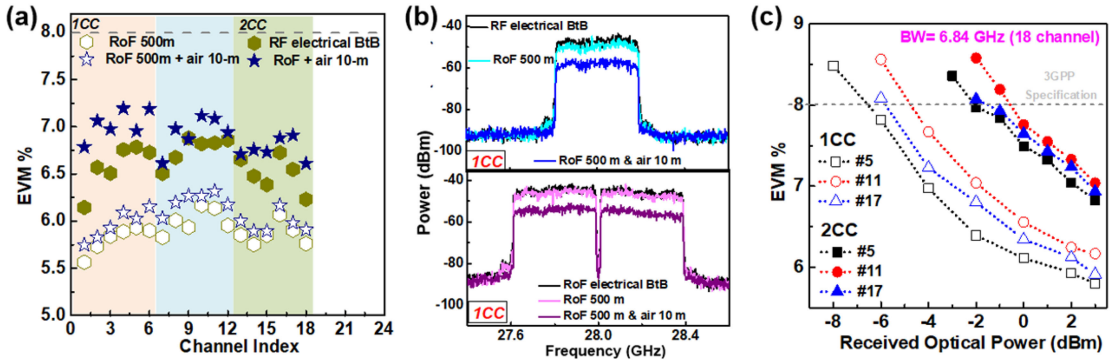

Fig. 7. (a) EVM performances under different transmission stages. (b) The received RF spectra at 28 GHz for the 1CC and 2CC cases. (c) EVMs as a function of received optical power for different channels under the 1CC and 2CC conditions.

On the other hand, we found that it was possible to achieve wireless transmission with the 2CC condition if we reduced the number of channels to 18. In this case, the total bandwidth and the corresponding capacity became 6.84 GHz and 25.65 Gbps. Note that we performed pre-emphasis again based on the 18-channel response. Since the number of channels was simply reduced, the average EVM after the 500-m RoF link could be improved to 6.7%, as illustrated in Fig. 7(a). Fig. 7(b) compares the received RF spectra at 28 GHz for both the 1CC and 2CC cases in the electrical BtB state and after the 500-m RoF and 10-m wireless transmission. Although we had a 10-dB free-space propagation loss, the effect could be minimized by employing an RF amplifier, and only a small SNR degradation was observed. This resulted in a small EVM increase to 6.1% and 6.9%, as also shown in Fig. 7(a). On the other hand, the EVM versus received optical power in the RoF link is illustrated in Fig. 7(c). To meet the 8-% criterion, a minimum received optical power of -6.5 dB was needed at channel #5 in the 1CC case. In this case, the power budget was found to be 9.5 dB. However, the minimum power was increased to -2.1 dBm in the 2CC case. In this case, the power budget was decreased to 5.1 dB. On the other hand, the received power budgets were found to be 3.5 and 4.6 dB for channel #11 and #17, respectively in the 2CC condition.

V. Conclusion

A proof-of-concept of an end-to-end analog MFH link based on the hybrid IFoF/A-RoF link has been presented for a future 5G wireless system. We successfully demonstrated real-time transmission of multi-channel 5G NR signals and achieved a total system capacity of 34.2 Gbps (24×0.38 GHz×3.75 bps/Hz) over 20-km broadband IFoF, 1-km narrowband IFoF, 500-m RoF, and 10-m free-space links. By using pre-emphasis, the degradation of frequency response stemming from RF devices and dispersion-induced power fading can be compensated at the broadband IFoF link. We also employed a digital demultiplexer to perform channel selection after the narrowband IFoF link.

These results show the feasibility of transmitting 1CC (400-MHz) and 2CC (800-MHz) signals over the hybrid IFoF/RoF links. We further achieved 2CC fiber/wireless transmission by reducing the IF modulation bandwidth to 6.84 GHz. We confirmed that all the EVM values after the wireless link satisfied the 8% criterion. The obtained results showed the potential of the hybrid IFoF/A-RoF system for a high-capacity 5G MFH system.

REFERENCES

[1] Ericsson, "The 5G consumer business case," Aug. 2018, [Online]. Available: https://www.ericsson.com/en/blog/2018/2/5-things-you-need-to-know-about-the-5g-consumer-business-case.

[2] 5G PPP, "5G vision," White Paper, Feb. 2015. [Online]. Available: https://5g-ppp.eu/wp-content/uploads/2015/02/5G-Vision-Brochure-v1.pdf

[3] J. G. Andrews *et al.*, "What will 5G be?," *IEEE J. Sel. Areas Commun.*, vol. 32, no. 6, pp. 1065–1082, Jun. 2014.

[4] *IMT Vision Framework and Overall Objectives of the Future Development of IMT for 2020 and Beyond*, ITU-R Standard Rec. M.2083-0, International Telecommunication Union, Geneva, Switzerland, Sep. 2015.

[5] S. E. Alavi *et al.*, "Towards 5G: A photonic based millimeter wave signal generation for applying in 5G access fronthaul," *Sci. Rep.*, vol. 6, 2016, Art. no. 19891.

[6] K. Tanaka and A. Agata, "Next-generation optical access networks for CRAN," in *Proc. Opt. Fiber Commun. Conf.*, 2015, Paper Tu2E.1.

[7] K. Tanaka, H.-Y. Kao, S. Ishimura, K. Nishimura, T. Kawanishi, and M. Suzuki, "Cascaded IF-over-fiber links with hybrid signal processing for analog mobile Fronthaul," *J. Lightw. Technol.*, vol. 38, no. 20, pp. 5656–5667, 2020.

[8] 3GPP Technical specification (TS) 38.101-1 Release 15 (2018).

[9] M. Xu, F. Lu, J. Wang, L. Cheng, D. Guidotti, and G.-K. Chang, "Key technologies for next-generation digital RoF mobile fronthaul with statistical data compression and multiband modulation," *J. Lightw. Technol.*, vol. 35, pp. 1647–1656, 2017.

[10] A. Saadani *et al.*, "Digital radio over fiber for LTE-advanced: Opportunities and challenges," in *Proc. Int. Conf. Opt. Netw. Des. Model.*, 2013, pp. 194–199.

[11] S. Ishimura *et al.*, "Broadband IF-over-fiber transmission with parallel IM/PM transmitter overcoming dispersion-induced RF power fading for high-capacity mobile fronthaul links," *IEEE Photon. J.*, vol. 10, no. 1, Feb. 2018, Art. no. 7900609.

[12] China Mobile Research Institute, Beijing, China, "Next generation fronthaul interface," White Paper, 2015. [Online]. Available: http://labs.chinamobile.com/cran

[13] M. Suzuki *et al.*, "Optical and wireless integrated technologies for future mobile networks," in *Proc. 19th Int. Conf. Transparent Opt. Netw*., 2017, pp. 1–4.

[14] Study on New Radio Access Technology; Radio access architecture and interfaces (Release 14), 3GPP TR 38.801 V2.0.0, 2017.

[15] D. A. A. Mello *et al.*, "Spectrally efficient fronthaul architectures for a cost-effective 5G C-RAN," in *Proc. Int. Conf. Transparent Opt. Netw.*, 2016, Paper We.C2.4.

[16] Y. Tian, K.-L. Lee, C. Lim, and A. Nirmalathas, "60 GHz analog radio-over-fiber fronthaul investigations," *J. Lightw. Technol.*, vol. 35, no. 19, pp. 4304–4310. 2017.

[17] B. G. Kim, S. H. Bae, H. Kim, and Y. C. Chung, "DSP-based CSO cancellation technique for RoF transmission system implemented by using directly modulated laser," *Opt. Exp.*, vol. 25, pp. 12152–12160, 2017.

[18] X. Liu, H. Zheng, N. Chand, and F. Effenberger, "CPRI-compatible efficient mobile fronthaul transmission via equalized TDMA achieving 256 Gb/s CPRI-equivalent data rate in a single 10-GHz-bandwidth IM-DD channel," in *Proc. Opt. Fiber Commun. Conf.*, 2016, Paper W1H.3.

[19] S.-H. Cho *et al.*, "Cost-effective next generation mobile fronthaul architecture with multi-IF carrier transmission scheme," in *Proc. Opt. Fiber Commun. Conf.*, 2014, Paper Tu2B.6.

[20] N. Shibata *et al.*, "256-QAM 8 wireless signal transmission with DSP-assisted analog RoF for mobile front-haul in LTE-B," in *Proc. Optoelectron. Commun. Conf. Aust. Conf. Opt. Fibre Technol.*, 2014, pp. 129–131.

[21] X. Liu, H. Zeng, N. Chand, and F. Effenberger, "Efficient mobile fronthaul via DSP-based channel aggregation," *J. Lightw. Technol.*, vol. 34, no. 6, pp. 1556–1564, 2016.

[22] S. Ishimura *et al.*, "1.032-Tb/s CPRI-equivalent rate IF-over-fiber transmission using a parallel IM/PM transmitter for high-capacity mobile fronthaul links," *J. Lightw. Technol.*, vol. 46, no. 8, pp. 1478–1484, 2018.

[23] H.-Y. Kao *et al.*, "End-to-end demonstration based on hybrid IFoF and analogue RoF/RoMMF links for 5G access/in-building network system," in *Proc. Eur. Conf. Opt. Commun.*, 2020, Paper Tu1G-7.

[24] P. Guan *et al.*, "Novel hybrid radio-over-fiber transmitter for generation of flexible combination of WDM-ROF/WDM channels," in *Proc. Opt. Fiber Commun. Conf.*, 2019, Paper W1I.6.

[25] X. Liu *et al.*, "Real-time demonstration of over 20Gbps V- and W-band wireless transmission capacity in one OFDM-RoF system," in *Proc. Opt. Fiber Commun. Conf.*, 2017, Paper M3E.3.

[26] N. Argyris *et al.*, "A 5G mmWave fiber-wireless IFoF analog mobile fronthaul link with up to 24-Gb/s multiband wireless capacity," *J. Lightw. Technol.*, vol. 37, no. 12, pp. 2883–2891, 2019.

[27] P. T. Dat *et al.*, "Full-duplex transmission of nyquist-SCM signal over a seamless bidirectional fiber–wireless system in W-Band," in *Proc. Opt. Fiber Commun. Conf.*, 2019, Paper W1I.5.

[28] C. Browning, A. Delmade, Y. Lin, D. H. Geuzebroek, and L. P. Barry," Optical heterodyne millimeter-wave analog radio-over-fiber with photonic integrated tunable lasers," in *Proc. Opt. Fiber Commun. Conf.*, 2019, Paper W1I.4.

[29] M. Sung *et al.*, "Demonstration of IFoF-based mobile fronthaul in 5G prototype with 28-GHz millimeter wave," *J. Lightw. Technol.*, vol. 36, no. 2, pp. 601–609, 2018.

[30] H. R. D. Filgueiras, R. M. Borges, M. C. Melo, T. H. Brandão, and A. C. Sodré, "Dual-band wireless fronthaul using a FSS-based focal-point/cassegrain antenna assisted by an optical midhaul," *IEEE Access*, vol. 7, pp. 112578–112587, 2019.

[31] A. Tsakyridis *et al.*, "Reconfigurable fiber wireless IFoF fronthaul with 60 GHz phased array antenna and silicon photonic ROADM for 5G mmWave C-RANs," *IEEE J. Sel. Areas Commun.*, vol. 39, no. 9, pp. 2816–2826, Sep. 2021.

[32] K. Tanaka *et al.*, "Bidirectional IFoF mobile fronthaul with DSP-based channel multiplexer and demultiplexer," in *Proc. Optoelectron. Commun. Conf.*, 2021, pp. 1–3.